Diagnostic Accuracy Study

Medicine®

OPEN

Correlation of tumor uptake on breast-specific gamma imaging and fluorodeoxyglucose PET/CT with molecular subtypes of breast cancer

Soo Jin Lee, MD, PhD[a], Min Sung Chung, MD, PhD[b,*], Su-Jin Shin, MD, PhD[c], Yun Young Choi, MD, PhD[a,*]

Abstract

Mechanisms of technetium-99m sesta-methoxyisobutylisonitrile (sestamibi) and ^{18}F-fluorodeoxyglucose (FDG) uptake by tumor are different. The purpose of this study was to investigate the association between the tumor uptake of these 2 tracers in invasive ductal carcinoma and to examine thecorrelation of uptake of each tracer with prognostic factors and tumor molecular subtypes.

A total of 96 patients with invasive ductal carcinoma who underwent preoperative breast-specific gamma imaging and FDG positron-emission tomography/computed tomography were retrospectively enrolled. Tumor-to-background ratio (TBR) of sestamibi and maximum standardized uptake value (SUV_{max}) of FDG were correlated with each other. Each of them was then compared with prognostic factors and molecular subtypes.

In all tumors, there was a moderate positive correlation between TBR and SUV_{max} ($r = 0.520$, $P < .001$). Both TBR and SUV_{max} were significantly correlated with tumor size, incidence of axillary lymph node metastasis, histologic grade, estrogen receptor, progesterone receptor status, and Ki-67.

There is a moderate degree of association between TBR of sestamibi and SUV_{max} of FDG in the invasive breast cancer. Two imaging indexes showed the similar tendency related with prognostic factors and molecular subtypes. While both TBR and SUV_{max} were significantly different between luminal A and nonluminal A tumors, neither of them had high enough sensitivity or specificity to obviate pathologic and molecular diagnosis.

Abbreviations: ANOVA = analysis of variance, BIRAD = breast imaging reportingand data system, BSGI = breast-specific gamma imaging, CC = craniocaudal, ER = estrogen receptor, FDG = fluorodeoxyglucose, HER2 = human epithelial growth factor receptor 2, HG = histologic grade, IDC = invasive ductal cancer, IHC = immunohistochemistry, ILC = invasive lobular cancer, MLO = mediolateral oblique, PET/CT = positron-emission tomography/computed tomography, PR = progesterone receptor, ROI = region-of-interest, sestamibi = sesta-methoxyisobutylisonitrile, SUV = standardized uptake value, ^{99m}Tc = technetium-99m, TBR = tumor-to-background ratio, TNBC = triple-negative breast cancer.

Keywords: technetium-99m sesta-methoxyisobutylisonitrile, breast cancer, breast-specific gamma imaging, breast-specific gamma imaging, fluorodeoxyglucose

1. Introduction

Breast cancer is a heterogeneous disease with various pathologic and molecular features.[1] The prognosis and therapeutic decision making of breast cancer are known to depend on the classic immunohistochemistry (IHC) markers: estrogen receptor (ER), progesterone receptor (PR), and human epidermal growth factor receptor 2 (HER2). Proliferative activity, represented by Ki-67, reflects the aggressive behavior of breast cancer. Subgroup classification according to the combination of expression of ER, PR, HER2, and Ki-67 was proposed as a new index for prognostic prediction. The current pathology-based classification of subtypes presented in the St Gallen International Expert Consensus on 2015 concerned prognosis and classified breast cancers into 4 types: luminal A, luminal B, HER2, and triple-negative cancer (TNBC) types.[2]

Fluorine-18 fluorodeoxyglucose (FDG) positron-emission tomography/computed tomography (PET/CT) is a well-known molecular imaging technique used to evaluate oncologic diseases. The maximum standardized uptake value (SUV_{max}) of FDG as a semiquantitative index has been shown to correlate with prognostic factors in breast cancer and to be useful for assessing the response to chemotherapy.[3,4] Recent studies have reported that SUV_{max} differs among the molecular subtypes of breast cancer.[5,6]

Breast-specific gamma imaging (BSGI) using technetium-99m (^{99m}Tc) sesta-methoxyisobutylisonitrile (sestamibi) is reported to have a high diagnostic performance as an excellent adjunct modality to mammography for detecting breast cancer.[7] Sestamibi uptake by tumor is affected by angiogenesis, regional blood perfusion, and mitochondrial membrane potentials,[8] while FDG uptake reflects glucose utilization. Thus, the 2 tracers reflect different functional properties of tumor. However, similar to SUV_{max} of FDG on PET/CT, the tumor-to-background ratio

Editor: Michael Masoomi.

MSC and YYC contributed equally as the corresponding authors.

This work was carried out with the support of the research fund of Hanyang University (HY-2017-N).

The authors have no conflicts of interest to disclose.

[a] Department of Nuclear Medicine, [b] Department of Surgery, [c] Department of Pathology, Hanyang University Medical Center, Seoul, Korea.

[*] Correspondence: Yun Young Choi, Department of Nuclear Medicine, Hanyang University Medical Center, 222-1 Wangsimni-ro, Seongdong-gu, Seoul 04763, Korea (e-mail: ychoi@hanyang.ac.kr); Min Sung Chung, Department of Surgery, Hanyang University Medical Center, 222-1 Wangsimni-ro, Seongdong-gu, Seoul 04763, Korea (e-mail: bovie@hanyang.ac.kr).

Medicine (2018) 97:43(e12840)

Received: 20 June 2018 / Accepted: 22 September 2018

http://dx.doi.org/10.1097/MD.0000000000012840

(TBR) of sestamibi on BSGI has also been shown to predict the prognosis of breast cancer.[9]

The purpose of this study was to investigate: the association between sestamibi uptake and FDG uptake in the same tumor and the relationship of each tracer's tumor uptake with prognostic factors and subtypes of invasive breast cancer.

2. Materials and methods

2.1. Patients

This retrospective study was approved by the Institutional Review Board, and the need for informed written consent was waived. Patients with newly diagnosed invasive ductal cancer (IDC) between January 2014 and September 2016 were consecutively enrolled. Following exclusion of patients with tumor size <1 cm to avoid errors due to the partial volume effect, a total of 96 patients (94 with unilateral breast cancer and 2 with bilateral breast cancer) were enrolled in this study. In cases of multifocal cancers either unilateral or bilateral, the largest tumor was included for each patient.

2.2. Initial workup (biopsy and imaging)

All 96 patients had biopsy. Also, all patients underwent both sestamibi BSGI and FDG PET/CT for initial staging workup on 2 different days. BSGI was performed before biopsy in 25 patients and after biopsy in 71 patients. PET/CT was performed before biopsy in 9 patients and after biopsy in 87 patients. If BSGI or PET/CT was performed after biopsy, the minimum interval between biopsy and imaging was 7 days in an effort to avoid the effects of post-biopsy inflammation as much as possible.

2.3. Treatments

After the initial workup, 80 patients underwent surgical resection without preceding neoadjuvant or palliative chemotherapy; 9 patients were first treated with neoadjuvant chemotherapy followed by surgical resection; 5 patients who were diagnosed with distant metastasis were treated with palliative chemotherapy followed by surgical resection; 1 patient was treated with palliative chemotherapy alone; and the remaining 1 patient did not have any medical or surgical treatment after the initial staging workup.

2.4. BSGI protocol

Patients underwent BSGI with a high-resolution, small-field-of-view system (Dilon 6800; Dilon Technologies, Newport News, VA). Imaging was performed 10 minutes after intravenous injection of ^{99m}Tc-sestamibi (555 MBq) into the arm contralateral to the breast with the suspected lesion or the leg if bilateral breast cancer was suspected. Patients were in a seated position during the study. Craniocaudal (CC) and mediolateral oblique (MLO) images of both breasts were obtained. A low-energy, high-resolution collimator was used, and the energy window was centered on 140 keV ± 10%. Each planar image was acquired for 90,000 counts; the acquisition time for each image ranged from 5 to 8 minutes.

2.5. FDG PET/CT protocol

Patients fasted for more than 8 hours before PET/CT imaging. Blood glucose level was measured prior to FDG injection and confirmed to be <180 mg/dL in all patients. PET scans were started approximately 60 minutes after FDG injection (5.14 MBq/kg; average, 316 ± 49 MBq). All scans were performed using an integrated PET/CT scanner (Biograph 6; Siemens Healthcare, Knoxville, TN). A CT scan (110 kVp, 120 mAs) of 5 mm section thickness was performed for attenuation correction and lesion localization, and emission images were obtained from the skull base to the proximal thigh for 2.5 minutes per bed. PET images were reconstructed on 168 × 168 matrices using a standard iterative algorithm (OSEM).

2.6. Measurement of 2 imaging indexes (TBR and SUV_{max})

Two board-certified nuclear medicine physicians reviewed both BSGI and FDG PET/CT images. The BSGI data were classified into 5 categories according to the 2010 guidelines of the Breast Imaging Reporting and Data System (BIRADS) of the Society and Nuclear Medicine and Molecular Imaging.[10] Scores of 1, 2, and 3were classified as negative, and scores of 4 and 5were defined as positive. The scores were visually assessed by consensus between the 2 readers. In this study, a positive BSGI scan was observed in 87 (90.6%) of the 96 patients.

The TBR was obtained from each positive scan. First, a 2-cm region-of-interest (ROI) was placed over focally increased uptake representing the tumor; the maximum pixel count was used as tumor uptake of sestamibi. Second, three 2-cm ROIs were drawn within the breast parenchyma between the nipple and the base of the breast as shown in Figure 1; the mean pixel count from all 3 ROIs was used as background activity. Then, the TBR was calculated by dividing the maximum pixel count of the tumor by the mean pixel count of the background. Between 2 TBRs obtained from CC and MLO images, the higher TBR was selected for analysis. When the tumor could not be visually distinguished from normal breast tissue, a TBR of 1 was assigned.

The SUV_{max} on PET/CT for each tumor was obtained by drawing a volume of interest over the most intense area of FDG uptake by the tumor. If the tumor could not be visibly distinguished from background breast tissue, a volume of interest drawn to enclose the whole tumor lesion on the integrated CT was used to measure the SUV_{max}.

2.7. Pathologic and molecular diagnosis

Specimens for histopathologic analysis were obtained from surgical resection in 80 patients who did not receive any neoadjuvant or palliative chemotherapy. For 15 patients who received neoadjuvant or palliative chemotherapy and one patient who had no surgery, the specimens from core needle biopsy or gun biopsy atinitial diagnosis were used. The following parameters were retrieved from the report: histologic type; tumor size; metastasis to axillary lymph nodes; expression of ER, PR, and HER2; and Ki-67 index.

Tumor size was defined by the largest diameter in the surgical specimen or measured by MRI in patients treated with neoadjuvant chemotherapy. ER, PR, and HER2 expressions were interpreted according to the guidelines of ER/PR/HER2 testing in breast cancer, as outlined by the American Society of Clinical Oncology/College of American Pathologists.[11] ER and PR positivity were defined as 10% or more of the tumor cells with an indication of nuclear positivity according to the Allred scoring system.

Tumors were considered HER2 positive if they received a score of 3+ based on IHC. An IHC tumor score of 2+ warranted confirmation of HER2 expression by fluorescent in situ hybridization.

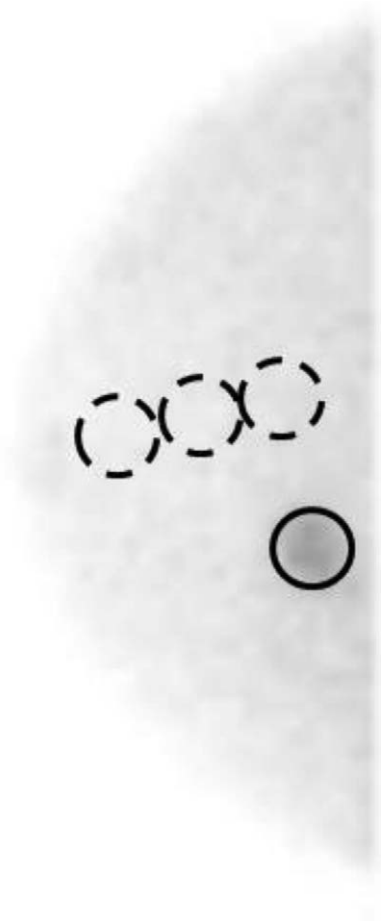

Figure 1. An example of a tumor-to-background ratio measurement on the craniocaudal image of breast-specific gamma imaging. The solid circle is placed on the tumor and three region-of-interests were drawn as shown between the nipple and the base of the breast.

The Ki-67 index was determined by IHC and recorded as a percentage.

Tumors were categorized into four subtypes[2]: luminal A (ER positive and/or PR positive, HER2 negative, and Ki-67 < 14%); luminal B (ER positive and/or PR positive, HER2 negative, and Ki-67 ≥ 14% or ER positive and/or PR positive, HER2 positive, and any Ki-67); HER2 positive (ER negative, PR negative, and HER2 positive), and triple negative (ER negative, PR negative, and HER2 negative).

2.8. Statistical analyses

All data were expressed as mean ± standard deviation (SD) or median and 95% confidence interval (CI), as appropriate. Independent *t* test for bimodal variables and analysis of variance (ANOVA) test and Kruskal–Wallis test with post hoc test for multiple variables were used to compare the TBR or SUV_{max} with prognostic factors and subtypes. Multiple regression analysis was performed using histologic factors; significant independent factors were determined by *P*-values <.05 in the univariable analysis. Receiver-operating characteristic (ROC) curve analysis was used to determine the diagnostic performance of TBR in identifying luminal A subtype.

Correlation analyses were performed using either Spearman correlation test. Spearman coefficients (*r*) were used to measure the strength of correlation between TBR and SUV_{max}, between each imaging index and Ki-67, and between each imaging index. Partial correlation analysis was performed, when deemed necessary. Spearman correlation coefficients (*r*) of >0.59, between 0.4 and 0.59, and <0.4 were considered a strong positive, moderate positive, and weak positive correlation, respectively. Statistical analyses were performed using commercial software packages (SPSS version 19; IBM, Chicago, IL), and *P*-values <.05 were considered statistically significant.

3. Results

3.1. Patient and tumor characteristics

Characteristics of 96 female patients are summarized in Table 1. The mean age was 53.7 ± 10.9 years, ranging from 30 to 85. The histologic types included IDC only (n = 89), IDC with invasive lobular cancer (ILC) (n = 5), IDC with micropapillary cancer (n = 1), and IDC with mucinous cancer (n = 1). The median size of the tumors was 2.6 cm, ranging from 1.1 to 10.2 (95% CI: 2.3–3.0). T1 was the most common T stage, (n = 48), followed by T2 (n = 37) and T3 (n = 11). A total of 36 patients had axillary lymph node metastasis, and 5 patients had distant metastasis. Regarding the subtypes, luminal A was the most common subtype (n = 43), followed by luminal B (n = 16), HER2 (n = 15), and TNBC (n = 22).

3.2. Correlation between TBR and SUV_{max}

There was a moderate, significant correlation between TBR and SUV_{max} when patients with all subtypes were combined (Fig. 2; $r = 0.520$, $P < .001$). On a subgroup analysis according to subtypes, there was a moderate, significant correlation between TBR and SUV_{max} in HER2 subgroup ($r = 0.675$, $P = .006$), but

Table 1

Patient characteristics.

Characteristics	Number	%
Age, years (range)	53.7 ± 10.9 (30–85)	
Number of tumors	96	
Histology		
IDC only	89	92.8
IDC with invasive lobular carcinoma	5	5.2
IDC with micropapillary carcinoma	1	1.0
IDC with mucinous carcinoma	1	1.0
Tumor size, cm	2.6 (1.1–10.2)	
Clinical T stage		
T1 (1 cm≤)	48	49.0
T2	37	38.5
T3	11	11.5
Axillary lymph node		
Negative	60	62.5
Positive	36	37.5
Distant metastasis		
Negative	91	94.8
Positive	5	5.2
Subtype		
Luminal A	43	44.8
Luminal B	16	16.7
HER2	15	15.6
TNBC	22	22.9

HER2 = human epidermal growth factor receptor 2, IDC = invasive ductal carcinoma, TNBC = triple-negative breast cancer.

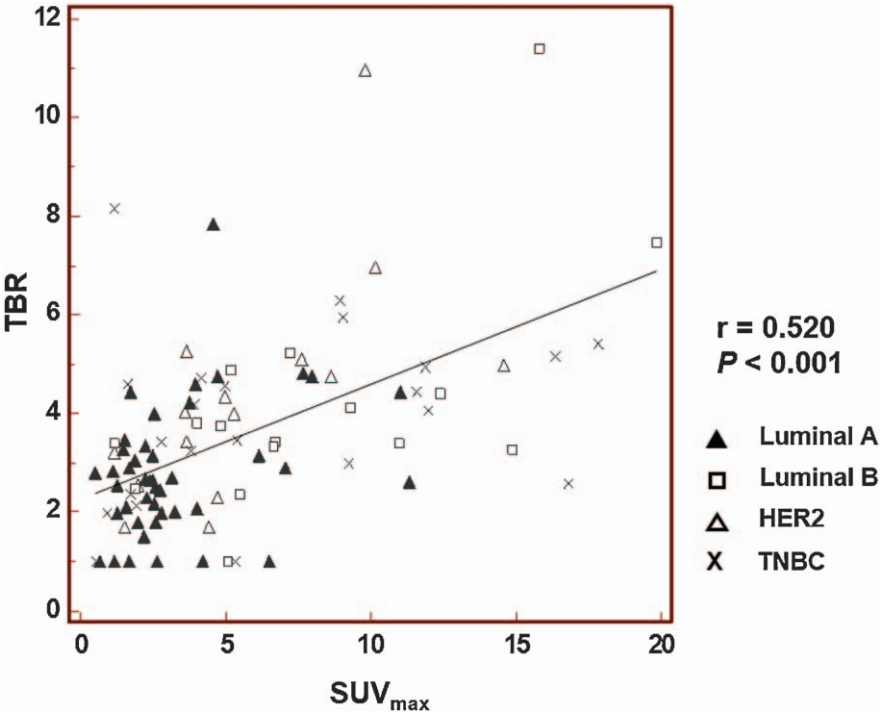

Figure 2. Correlation between tumor-to-background ratio (TBR) and maximum standardized uptake value (SUV_{max}) in all molecular subtypes combined.

not in other subgroups ($r=0.237$, $P=.076$ for luminal A; $r=0.478$, $P=.061$ for luminal B; $r=0.478$, $P=.061$ for TNBC).

3.3. Correlation of TBR and SUV_{max} with tumor variables

Table 2 shows the summarized results of the correlation between the 2 imaging indexes and tumor variables. On univariable analysis, both TBR and SUV_{max} were significantly higher in patients with poor prognostic factors such as larger tumor size, the presence of axillary lymph node metastasis, higher histologic grade, negative ER and PR status, and higher Ki-67 index (≥14%). On multivariable analysis, only tumor size and Ki-67 were found to be significantly correlated with both imaging indexes.

Table 2

Correlations between various tumor variables and two imaging indexes (TBR and SUV_{max}).

Characteristics	No.	TBR	P_{TBR}*	P_{TBR}†	SUV_{max}	P_{SUVmax}*	P_{SUVmax}†
Tumor size (cm)							
$1 \leq x \leq 2$	48	2.8±1.4	<.001	.001	3.5 (2.7–4.6)	<.001	<.001
>2	48	4.3±2.1			7.1 (5.9–8.6)		
Axillary lymph node							
Negative	60	3.2±1.7	.008		4.2 (3.3–5.1)	.002	
Positive	36	4.2±2.1			7.3 (5.7–8.9)		
Histologic grade							
1	18	3.0±0.9	.035		3.3 (2.5–4.2)	.001	
2 and 3	78	3.7±2.1			5.8 (4.8–6.8)		
ER							
Negative	42	4.0±1.9	.029		6.5 (5.2–8.1)	.019	
Positive	54	3.2±1.9			4.4 (3.4–5.5)		
PR							
Negative	44	4.2±1.9	.004		6.7 (5.3–8.1)	.008	
Positive	52	3.0±1.7			4.2 (3.3–5.4)		
HER2							
Negative	74	3.4±1.8	.145		5.1 (4.1–6.2)	.335	
Positive	22	4.1±2.1			6.1 (4.6–8.0)		
Ki-67							
Low (<14%)	51	2.9±1.4	.001	.001	3.5 (2.9–4.2)	<.001	<.001
High (≥14%)	45	4.3±2.2			7.4 (5.9–8.9)		

Data are presented as mean±standard deviation for TBR and median values (confidence interval) for SUV_{max}.

ER = estrogen receptor, HER2 = human epidermal growth factor receptor 2, PR = progesterone receptor, SUV_{max} = maximum standardized uptake value, TBR = tumor-to-background ratio.

* Univariable analysis.

† Multivariable analysis.

Table 3

Molecular subtypes and TBR of sestamibi and SUV_{max} of fluorodeoxyglucose.

Characteristics	No.	TBR	P_{TBR}	SUV_{max}	P_{SUVmax}
All					
Luminal A	43	2.8±1.4	.006	3.3 (2.7–4.1)	.001
Luminal B	16	4.2±2.4		8.2 (5.8–11.1)	
HER2	15	4.4 ±2.3		5.7 (3.9–7.7)	
TNBC	22	3.9±1.8		6.9 (4.5–9.3)	
Luminal A vs nonluminal A					
Luminal A	43	2.8±1.4	.001	3.3 (2.7–4.1)	<.001
Nonluminal A	53	4.1±2.1		7.0 (5.6–8.3)	
TNBC vs non-TNBC					
TNBC	22	3.9±1.8	.355	6.6 (4.2–0.0)	.141
Non-TNBC	74	3.5±1.9		5.0 (4.1–6.0)	

Data are presented as mean±standard deviation for TBR and median values (confidence interval) for SUV_{max}.
HER2=human epidermal growth factor receptor 2, sestamibi = sesta-methoxyisobutylisonitrile, SUV_{max} = maximum standardized uptake value, TBR=tumor to background ratio, TNBC=triple-negative breast cancer.

3.4. Correlation of TBR and SUV_{max} with molecular subtypes

Both imaging indexes were found to have a significant association with subtypes ($P=.006$ for TBR by ANOVA and $P=.001$ for SUV_{max} by Kruskal–Wallis test, Table 3); post-hoc tests showed a significant difference between luminal A and other subtypes.

When the subtypes were divided into luminal A and nonluminal A subgroups, both indexes were significantly lower in the luminal A than the nonluminal A subgroup ($P=.001$ for TBR and $P<.001$ for SUV_{max}). The mean TBR and median SUV_{max} values were 2.8±1.4 and 3.3 (95% CI 2.7–4.1)for luminal A and 4.1±2.1 and 7.0 (5.6–8.3) for nonluminal A subtypes, respectively. For prediction of the luminal A subtype, sensitivities and specificities were 73.6% and 72.1% at a cutoff TBR of 3.16 and 77.4% and 69.8% at a cutoff SUV_{max} of 3.24. The best area under the curve (AUC) was 0.720 for TBR and 0.736 for SUV_{max}.

On the contrary, when the subtypes were divided into TNBC and non-TNBC subgroups, there was no significant difference in either index between the 2 subgroups.

4. Discussion

We found that both TBR and SUV_{max} significantly correlated with some of the known prognostic factors. While both indexes correlated positively with larger tumor size, the presence of axillary lymph node metastasis, higher histologic grade, the negative status of ER and PR, and higher Ki-67 on univariable analysis, multivariable analysis showed the tumor size and Ki-67 to be only significant variables correlating with both indexes.

The 2 imaging indexes correlated with each other. When each of TBR and SUV_{max} was separately correlated with subtypes of breast cancer, both imaging indexes were found to be significantly different between luminal A and nonluminal A subgroups. Using the optimal cutoff values obtained from ROC analyses, the sensitivity and specificity of TBR for differentiating luminal A from nonluminal A types were 73.6% and 72.1%, respectively. Similarly, the sensitivity and specificity of a cutoff SUV_{max} of 3.24 for differentiating luminal A from nonluminal A types were 77.4% and 69.8%, respectively. This result is nearly identical to 79% sensitivity and 68% specificity using a cutoff SUV_{max} of 5.4 for the prediction of luminal A type recently reported by Miyake et al.[12] The difference in the optimal cutoff SUV_{max} might have resulted from the difference in PET/CT systems used.[13] Nonetheless, our results are consistent with Miyake et al's results and confirm that luminal A tumors have significantly lower FDG uptake than nonluminal A tumors. However, our view is slightly different from Miyake et al's; while they concluded that SUV_{max} had acceptable diagnostic performance, we do not believe that this level of sensitivity and specificity is high enough to make FDG-PET/CT an independent diagnostic test for identification of luminal A tumors. Likewise, 73.6% sensitivity and 72.1% specificity for the prediction of luminal A type using a cutoff TBR of 3.16 are also not sufficiently high.

The present study has limitations inherent to its retrospective nature. In most patients, BSGI or FDG PET/CT imaging could not be performed before biopsy due to 3rd-party reimbursement issues. However, we tried our best to wait a minimum of 1 week after the biopsy to minimize/avoid the effects of biopsy-related inflammation as acute inflammation would generally subside within several days. The pathologic examinations of surgically resected specimens indeed revealed virtually no neutrophils in tumor specimen except for a small number of neutrophils only at the biopsy site (detailed data not presented in Section 3). Further, SUV values in our study were lower than those of other investigators. It is unknown whether or not the difference in SUV values among studies is in part related to the presence of inflammation in 1 study vs other studies. Regardless, the fact that our SUVs were lower than those in other reports indirectly supports the lower likelihood of significant influence of biopsy-related inflammation on sestamibi or FDG uptake in our study.

Another issue that merits discussion is a selection of background activity. Underlying breast tissue density may vary among patients and so the accumulated counts. Therefore, the mean value for the background regions above and below the tumor region with the same proximity to the base of the breast could represent an optimal background activity. Unfortunately, it was not feasible to select such background regions consistently in all patients for various reasons, for example, tumors are located near the nipple or superficially in some patients (in whom ROIs could not be drawn above the tumor) or near the base of breast in others (in whom ROIs could not be drawn below the tumor). Instead, we tried to find a way to obtain background activity which is least affected by the breast density. In our previous study, we found that background activity obtained from the mean activity of three circular ROIs drawn within the breast parenchyma between the nipple and the base of the breast

(employed in our current paper as well) was not affected by the breast density. In summary, we believe that our study, despite some inherent limitations, has provided new information on uptake of sestamibi and FDG in the same breast cancers and their correlation with subtypes of breast cancer.

5. Conclusion

In patients with invasive breast cancer, there is a moderate degree of association between TBR of sestamibi and SUV_{max} of FDG in the same tumor. There appears to be a similar tendency in the relationship between the 2 imaging indexes and prognostic factors and molecular subtypes; both TBR and SUV_{max} positively correlated with poor prognostic factors, especially Ki-67. While both TBR and SUV_{max} were significantly different between luminal A and nonluminal A tumors, neither of them had high enough sensitivity or specificity to obviate pathologic and molecular diagnosis.

Author contributions

Conceptualization: Min Sung Chung.
Data curation: Yun Young Choi.
Formal analysis: Soo Jin Lee, Su-Jin Shin.
Investigation: Su-Jin Shin.
Methodology: Min Sung Chung, Yun Young Choi.
Supervision: Yun Young Choi.
Writing – original draft: Soo Jin Lee.
Writing – review & editing: Soo Jin Lee.
Soo Jin Lee orcid: 0000-0002-5600-1315.

References

[1] Perou CM, Sorlie T, Eisen MB, et al. Molecular portraits of human breast tumours. Nature 2000;406:747–52.
[2] Coates AS, Winer EP, Goldhirsch A, et al. Tailoring therapies–improving the management of early breast cancer: St Gallen International Expert Consensus on the Primary Therapy of Early Breast Cancer 2015. Ann Oncol 2015;26:1533–46.
[3] Groheux D, Giacchetti S, Moretti JL, et al. Correlation of high 18F-FDG uptake to clinical, pathological and biological prognostic factors in breast cancer. Eur J Nucl Med Mol Imaging 2011;38:426–35.
[4] Berriolo-Riedinger A, Touzery C, Riedinger JM, et al. [18F]FDG-PET predicts complete pathological response of breast cancer to neo-adjuvant chemotherapy. Eur J Nucl Med Mol Imaging 2007;34: 1915–24.
[5] Garcia Vicente AM, Soriano Castrejon A, Leon Martin A, et al. Molecular subtypes of breast cancer: metabolic correlation with (1)(8)F-FDG PET/CT. Eur J Nucl Med Mol Imaging 2013;40:1304–11.
[6] Kitajima K, Fukushima K, Miyoshi Y, et al. Association between (18)F-FDG uptake and molecular subtype of breast cancer. Eur J Nucl Med Mol Imaging 2015;42:1371–7.
[7] Sun Y, Wei W, Yang HW, et al. Clinical usefulness of breast-specific gamma imaging as an adjunct modality to mammography for diagnosis of breast cancer: a systemic review and meta-analysis. Eur J Nucl Med Mol Imaging 2013;40:450–63.
[8] Papantoniou V, Christodoulidou J, Papadaki E, et al. Uptake and washout of 99mTcV-dimercaptosuccinic acid and 99mTc-sestamibi in the assessment of histological type and grade in breast cancer. Nucl Med Commun 2002;23:461–7.
[9] Yoo J, Yoon HJ, Kim BS. Prognostic value of primary tumor SUVmax on F-18 FDG PET/CT compared with semi-quantitative tumor uptake on Tc-99m sestamibi breast-specific gamma imaging in invasive ductal breast cancer. Ann Nucl Med 2017;31:19–28.
[10] Goldsmith SJ. The SNM practice guideline on breast scintigraphy. J Nucl Med 2010;51:1823–4.
[11] Hammond ME, Hayes DF, Wolff AC, et al. American society of clinical oncology/college of American pathologists guideline recommendations for immunohistochemical testing of estrogen and progesterone receptors in breast cancer. J Oncol Pract 2010;6:195–7.
[12] Miyake KK, Nakamoto Y, Kanao S, et al. Journal Club: Diagnostic value of (18)F-FDG PET/CT and MRI in predicting the clinicopathologic subtypes of invasive breast cancer. AJR Am J Roentgenol 2014;203: 272–9.
[13] Park K, Ashlock R, Chang W, et al. High variation in standardized uptake values among PET systems from different manufacturers. J Nucl Med 2007;48:185P.